

Gene-expression profiling identifies distinct subclasses of core binding factor acute myeloid leukemia

Lars Bullinger,¹ Frank G. Rücker,¹ Stephan Kurz,¹ Juan Du,¹ Claudia Scholl,¹ Sandrine Sander,² Andrea Corbacioglu,¹ Claudio Lottaz,³ Jürgen Krauter,⁴ Stefan Fröhling,¹ Arnold Ganser,⁴ Richard F. Schlenk,¹ Konstanze Döhner,¹ Jonathan R. Pollack,⁵ and Hartmut Döhner¹

¹Department of Internal Medicine III, University of Ulm, Ulm, Germany; ²Department of Physiological Chemistry, University of Ulm, Ulm, Germany; ³Department for Computational Molecular Biology, Max-Planck-Institute for Molecular Genetics, Berlin, Germany; ⁴Department of Hematology, Hemostasis, Oncology, and Stem Cell Transplantation, Hannover Medical School, Hannover, Germany; and ⁵Department of Pathology, Stanford University, Palo Alto, CA

Core binding factor (CBF) leukemias, characterized by either *inv(16)/t(16;16)* or *t(8;21)*, constitute acute myeloid leukemia (AML) subgroups with favorable prognosis. However, there exists substantial biologic and clinical heterogeneity within these cytogenetic groups that is not fully reflected by the current classification system. To improve the molecular characterization we profiled gene expression in a large series (n = 93) of AML patients with CBF leukemia [*inv(16)*, n = 55; *t(8;21)*, n = 38]. By unsupervised hierarchical clustering we were able to define a sub-

group of CBF cases (n = 35) characterized by shorter overall survival times (P = .03). While there was no obvious correlation with fusion gene transcript levels, *FLT3* tyrosine kinase domain, *KIT*, and *NRAS* mutations, the newly defined *inv(16)/t(8;21)* subgroup was associated with elevated white blood cell counts and *FLT3* internal tandem duplications (P = .011 and P = .026, respectively). Supervised analyses of gene expression suggested alternative cooperating pathways leading to transformation. In the “favorable” CBF leukemias, antiapoptotic

mechanisms and deregulated mTOR signaling and, in the newly defined “unfavorable” subgroup, aberrant MAPK signaling and chemotherapy-resistance mechanisms might play a role. While the leukemogenic relevance of these signatures remains to be validated, their existence nevertheless supports a prognostically relevant biologic basis for the heterogeneity observed in CBF leukemia. (Blood. 2007; 110:1291-1300)

© 2007 by The American Society of Hematology

Introduction

Characterized by either *t(8;21)(q22;q22)* and its variants [abbreviated *t(8;21)*] or *inv(16)(p13q22)/t(16,16)(p13;q22)* [abbreviated *inv(16)*], core binding factor (CBF) acute myeloid leukemias (AMLs) have been shown to constitute AML subgroups with favorable prognosis.¹⁻³ However, the current World Health Organization classification^{4,5} does not fully reflect the biologic and clinical heterogeneity within these cytogenetically defined subgroups.

At the molecular level, *t(8;21)* and *inv(16)* result in the fusion genes *RUNX1/CBFA2T1* and *CBFB/MYH11*, respectively,⁶⁻⁸ that lead to the disruption of the CBF complex, a transcription factor complex involved in the regulation of hematopoiesis.⁹ The CBF complex consists of a heterodimer of the RUNX1 (formerly AML1) and the CBFB protein and normally activates a number of genes critical for normal myeloid development. In CBF AML, the fusion proteins act as dominant negative forms of the CBF, thereby impairing hematopoietic differentiation and predisposing to leukemic transformation.¹⁰ However, knock-in mouse models have demonstrated that *t(8;21)* and *inv(16)* by themselves are not sufficient to cause a leukemic phenotype^{11,12} and that additional aberrations were essential for the development of AML.^{11,13,14}

These findings suggest a multistep nature of leukemogenesis, a possible explanation for patients differing with respect to several biologic and clinical features, because almost one third of patients relapse within the first year following intensive chemotherapy.^{15,16}

Secondary chromosome abnormalities such as the commonly observed loss of a sex chromosome (-Y or -X), and/or deletions of the long arm of chromosome 9 in *t(8;21)*, and trisomies of chromosomes 22, 8, and 21 in *inv(16)*^{15,16} likely contribute to the heterogeneity of CBF leukemias. Recent molecular analyses have also provided important insights into the pathogenesis of myeloid disorders, and the commonly detected mutations of the *KIT* and *NRAS* genes as well as deregulated *CEBPA* expression have been identified as likely candidates for cooperating events in CBF AML.¹⁷ Furthermore, the identification of an alternatively spliced isoform of the *RUNX1/CBFA2T1* transcript may be involved in the development of *t(8;21)*-positive leukemias.¹⁸ However, despite this progress the molecular biology underlying CBF AML is still not fully understood.

Recently, DNA microarray technology-based gene-expression profiling (GEP) studies have shown the power of genomewide analysis to capture the molecular heterogeneity of AML.¹⁹⁻²² Interestingly, gene-expression analyses also captured the molecular variation within CBF leukemia showing that *t(8;21)* or *inv(16)* cases are not each tightly correlated, with each class, *t(8;21)* and *inv(16)*, being separated into mainly 2 groups.¹⁹ In agreement, Valk and colleagues also observed a molecular variation within their “homogeneously grouped” CBF cases using less stringent clustering criteria.²⁰ Distinct patterns of gene expression within each of the subgroups might reflect alternative cooperating mutations and/or

Submitted October 2, 2006; accepted April 22, 2007. Prepublished online as *Blood* First Edition paper, May 7, 2007; DOI 10.1182/blood-2006-10-049783.

The publication costs of this article were defrayed in part by page charge payment. Therefore, and solely to indicate this fact, this article is hereby marked “advertisement” in accordance with 18 USC section 1734.

The online version of this article contains a data supplement.

© 2007 by The American Society of Hematology

deregulated pathways leading to transformation, because the t(8;21) and inv(16) themselves are not sufficient for leukemogenesis.

Hence, we analyzed a large series (n = 93) of AML patients with CBF leukemia [inv(16), n = 55; t(8;21), n = 38] using DNA microarray technology and correlated findings with known collaborating aberrations in CBF AML like additional cytogenetic and molecular genetic aberrations in order to (1) provide a refined molecular characterization of CBF leukemia and to (2) get new insights into the biology of CBF leukemia. Here we report the results leading to the identification of clinically relevant subclasses, highlighting genes and pathways of potential pathogenic relevance that provide a basis for novel molecular targeted therapeutic approaches in CBF AML.

Patients, materials, and methods

Patients

The 93 samples (49 peripheral blood [PB] and 44 bone marrow [BM] specimens) from adult AML patients were provided by the German and Austrian AML Study Group (AMLSG), with patient informed consent obtained in accordance with the Declaration of Helsinki and institutional review board approval from all participating centers. Patients were entered into 1 of 3 AMLSG treatment protocols (AML HD93 and AML HD98-A for younger adults [age less than 60 years] and AML HD98-B for elderly patients [age 60 years and older], enrolled between November 1994 and March 2004). Patients less than 60 years of age (n = 78) received intensive induction and consolidation therapy, whereas elderly patients 60 years and older (n = 15) were treated less intensely (for protocol details, see Schlenk et al^{16,23}). Patient age at the time of diagnosis ranged from 19 to 73 years (median, 47 years). Clinical characteristics at the time of diagnosis were available for almost all cases as detailed in Table 1. Estimated median follow-up time for the patients with survival information (n = 89) was 52.5 months (95% confidence interval [CI], 47 to 59 months).

Cytogenetic and molecular genetic analyses

Conventional chromosome banding, fluorescence in situ hybridization (FISH), and *FLT3* mutational analysis (screening for internal tandem duplications [ITDs] and tyrosine kinase domain [TKD] mutations) were performed as previously described^{24,25} at the central reference laboratory of the German and Austrian AMLSG at our institution.

RUNX1/CBFA2T1 and *CBFB/MYH11* fusion gene transcript levels at the time of diagnosis were evaluated by quantitative reverse transcriptase-polymerase chain reaction (RT-PCR) as previously reported^{26,27} by using the following primers and probes: *RUNX1* primer 5'-AATCACAGTGGATGGGCC-3'; *CBFA2T1* primer 5'-TGCGTCTTCACATCCACAGG-3'; *RUNX1/CBFA2T1* probe 5'-FAM-CTGAGAAGCACTCCACAATGCCA-GACT-TAMRA-3'; *CBFB* primer 5'-AGGTCTCATCGGGAGGAAATG-3'; *MYH11* primer 5'-TCTTCATCTCCTCCATCTGGGT-3'; *CBFB/MYH11* probe 5'-FAM-CCATGAGCTGGAGAAGTCCAAGCG-TAMRA-3'.

Exemplary technical validation of microarray-based gene-expression findings was performed accordingly using the following primers and probes: *FOXO1A* forward 5'-CTCATGGATGGAGATACATTGGATTT-3'; *FOXO1A* reverse 5'-GGTGAAAGACATCTTTGGACTGCTT-3'; *FOXO1A* probe 5'-FAM-CTAACCTCAGCCTGACACCCAGCTAT-TAMRA-3'; *MLL5* forward 5'-GGGTTGATACAGCAGAGACGTC-3'; *MLL5* reverse 5'-GGATTTCTCACTACCACAGGGC-3'; *MLL5* probe 5'-FAM-TGGCTGCAGTTCCAGAACCAATCC-TAMRA-3'; *ETS1* forward 5'-CCGTACGTCCCCACTCCT-3'; *ETS1* reverse 5'-TGGAATGTG-CAGATGTCCCA-3'; and *ETS1* probe 5'-FAM-CGTCGATCTCAAG-CCGACTCTCACCAT-TAMRA-3'.

Screening for mutations in *KIT* and *NRAS* was performed by a denaturing high-performance liquid chromatography (dHPLC)-based method using a WAVE dHPLC-system (Transgenomic, Omaha, NE) as previously reported.²⁸ In brief, DNA isolation was performed as de-

Table 1. Distribution of factors by type of CBF AML at diagnosis

Factors at diagnosis	t(8;21); n = 38	inv(16); n = 55	P
Sex			
Male, no. (%)	28/38 (74)	31/55 (56)	—
Female, no. (%)	10/38 (26)	24/55 (44)	ns
Age			
No. of patients	36	53	—
Median, y (range)	50 (19-73)	42 (19-72)	.030
FAB subtype			
M2 (%)	23/34 (68)	2/51 (4)	< .001
M4 (%)	2/34 (6)	46/51 (90)	—
Other (%)	9/34 (26)	3/51 (6)	—
WBC			
No. of patients	36	51	—
Median, × 10 ⁹ /L (range)	13 (2-152)	36 (2-157)	.013
BM blast			
No. of patients	31	43	—
Median, % (range)	52 (6-90)	74 (10-100)	.014
Overall survival			
No. of patients	36	53	—
Median, d	1430	1661	ns
Additional cytogenetic aberrations			
None (%)	11/36 (31)	36/53 (68)	.001
Trisomy 8 (%)	3/36 (8)	8/53 (15)	ns
del(9q)-9 (%)	3/36 (8)	0/53 (0)	ns
Trisomy 22 (%)	0/36 (0)	6/53 (11)	.0761
-Y/males (%)	15/27 (56)	1/29 (3)	< .001
-X/females (%)	5/9 (56)	0/24 (0)	< .001
Other (%)	4/36 (11)	11/53 (21)	ns
Molecular genetic aberrations			
<i>FLT3</i> -ITD (%)	3/34 (9)	1/46 (2)	ns
<i>FLT3</i> -TKD (%)	2/31 (6)	7/45 (15)	ns
<i>KIT</i> mutation (%)	5/31 (16)	8/34 (24)	ns
Exon 8 (%)	2/31 (6)	4/34 (12)	ns
Exon 17 (%)	3/31 (10)	4/34 (12)	ns
<i>NRAS</i> mutation (%)	4/26 (15)	14/34 (41)	.057
Exon 1 (%)	2/26 (8)	6/34 (18)	ns
Exon 2 (%)	2/26 (8)	8/34 (24)	ns

ns indicates nonsignificant; —, not applicable.

scribed,^{24,29} and 50 ng DNA was used for all PCR amplifications with the previously published primers for *KIT* (exons 8 and 17) and *NRAS* (exon 1)³⁰ as well as *NRAS* (exon 2).³¹ Cycling conditions for mutation detection were as follows: 1 cycle, 2 minutes at 95°C; 35 cycles, 30 seconds at 94°C, 1 minute at 56°C, and 1 minute at 72°C; and 1 cycle, 10 minutes at 72°C. Heteroduplexes were then generated by means of a thermal cycler as follows: 95°C for 5 minutes; annealing/stabilization (starting at 94°C for 2 minutes with a -1°C touchdown until 45°C). Then, 5 to 10 μL of heteroduplexed PCR products were subsequently subjected to dHPLC. The elution temperature varied according to the analyzed products: *KIT* exon 8: 56°C; *KIT* exon 17: 56.2°C; *NRAS* exon 1: 59.8°C; *NRAS* exon 2: 58.2°C. The exact mutant sequence was confirmed for all samples showing an abnormal dHPLC profile. PCR products were purified followed by direct sequencing with the reverse primers using an ABI-PRISM310 genetic analyzer (Applied Biosystems, Foster City, CA).

Gene-expression profiling

Gene-expression profiling (GEP) was performed essentially as reported in all 93 samples using the previously described cDNA microarray platform (26 of these cases have already been published, whereas 67 cases were newly analyzed).¹⁹ The percentage of blasts for PB and BM samples prior to enrichment for leukemic cells by Ficoll-density gradient centrifugation ranged from 25% to 97% (median 53%) and 25% to 91% (median, 68%), respectively. Following enrichment all samples contained at least 80% leukemic cells. Fluorescence ratios were normalized by mean-centering genes for each array and then by mean-centering each gene across all arrays

within a large AML data set ($n = 260$). For subsequent analyses, we only included well-measured genes whose expression varied as determined by signal intensity over background greater than 2-fold in either test or reference channel in at least 75% of samples and 4-fold ratio variation from the mean in at least 2 samples; 8556 genes met these criteria. The complete gene-expression microarray data set is available at the Stanford Microarray Database³² and the filtered data set is provided as Table S1 (available on the *Blood* website; see the Supplemental Materials link at the top of the online article). For hierarchical clustering, we applied average-linkage hierarchical clustering and visualized results using TreeView.³³

Array CGH

For a subset of 58 cases [$t(8;21)$, $n = 29$; $inv(16)$, $n = 29$] array comparative genomic hybridization (CGH) experiments were performed as previously described using an 8k BAC/PAC microarray platform.³⁴ Fluorescence ratios were normalized using the median of the fluorescence ratios computed as \log_2 values from the DNA control fragments spanning the whole genome. For each individual experiment the cutoff level was determined by using an individual set of balanced clones that was used to calculate the mean and standard deviations. We then defined the cutoff level as $\text{mean} \pm 3$ times the standard deviation. Frequently affected regions recently detected as copy number polymorphisms were excluded from data analysis.^{35,36} Table S2 provides the entire normalized array CGH data set. Parallel analysis of gene-expression and array CGH data were performed as previously described.^{34,37} Map positions for arrayed cDNA clones were assigned using the National Center for Biotechnology Information (NCBI) May 2005 genome assembly accessed through the University of California Santa Cruz (UCSC) genome browser. In this way, approximately 35 000 arrayed clones representing 18 000 unique genes could be assigned map positions.

Data analysis

To evaluate the robustness of our hierarchical clusters, we used the R (reproducibility) measure³⁸ based on perturbing the expression data with gaussian noise, reclustering, and measuring the similarity of the new clusters to the original clusters. The perturbation and reclustering was done 100 times. For each pair of samples in a cluster of the original data, the R measure is the proportion of the time they stay in the same cluster after perturbation and reclustering. The R measure is expressed for each original cluster as an average over all pairs of samples and all perturbations and reclustering.

For 2-class supervised analyses, we identified genes that were differentially expressed among the 2 classes by using the significance analysis of microarrays (SAM) method,³⁹ which uses a modified t test statistic, with sample-label permutations to evaluate statistical significance. For class prediction we performed the prediction analysis for microarrays (PAM) method⁴⁰ based on nearest shrunken centroids to define a cross-validated gene-expression predictor for the cluster-defined CBF classes.

We identified gene ontology (GO) groups of genes whose expression was differentially regulated among the classes by computing the number of genes represented on the microarray in the respective GO group and the statistical significance P value for each gene in the group. These P values reflect differential expression among classes and were computed based on random variance t tests.⁴¹ For each GO group, 2 statistics were computed that summarize the P values for genes in the group: the Fisher (LS) statistic and the Kolmogorov-Smirnov (KS) statistic.⁴² We considered a GO category significantly differentially regulated if the significance level was less than .005. All GO categories with between 5 and 100 genes represented on the array were considered with some of the categories showing an overlap. The same computational algorithm was used to identify groups of genes belonging to distinct BioCarta or KEGG pathways whose expression was differentially regulated among the classes.

Survival times and censored waiting times measured from the date of diagnosis were plotted with Kaplan-Meier estimates. Cumulative incidence of relapse (CIR) and cumulative incidence of death (CID), their SE, and differences between groups were estimated according to Gray.⁴³ The median duration of follow-up was calculated according to the method of Korn.⁴⁴ Groupwise comparisons of the distributions of clinical and laboratory variables were performed using Fisher exact test and the

Cochran-Armitage test. All tests were 2-sided. An effect was considered significant if the (adjusted) P value was .05 or less. The analyses were performed using BRB-Array Tools Version 3.3.0 Beta_3 developed by Dr Richard Simon and Amy Peng Lam and using R, version 2.2.1.

Results

Gene-expression-based CBF subclass discovery

We profiled gene expression in 93 diagnostic peripheral blood and bone marrow samples using cDNA microarrays to survey the molecular variation of CBF AML. To explore the relationship among samples as well as the underlying patterns of gene expression, we performed an unsupervised 2-way hierarchical cluster analysis³³ using the 8556 genes whose expression varied most across samples (Figure 1A). In accordance with the previously observed heterogeneity within the CBF subgroups,¹⁹ the $t(8;21)$ and $inv(16)$ cases were not tightly correlated, with each cytogenetic class being segregated by the 2 main clusters defined by gene-expression profiling. Interestingly, within the larger cluster (group II) $t(8;21)$ and $inv(16)$ cases grouped mainly into 2 homogeneous $t(8;21)$ and $inv(16)$ classes, while in the other cluster (group I) $t(8;21)$ and $inv(16)$ cases were interspersed throughout, thereby forming one "mixed" $t(8;21)/inv(16)$ CBF subgroup (Figure 1A).

To evaluate the robustness of our hierarchical clusters we reclustered our samples 100 times using hierarchical clustering and measured the proportion of the time each sample stayed in the same cluster (Figure 2A). The consensus index of samples within consensus cluster no. 1 (group I) was $r = 0.836$, and samples in consensus cluster no. 2 (group II) were also tightly correlated ($r = 0.815$). We only observed that 2 "borderline cases" of group II were more often assigned to group I by reclustering the samples 100 times. Thus, these data suggest that group I and II represent robust classes.

Technical validation of microarray-based gene-expression findings was performed for selected genes, *FOXO1A*, *MLL5*, and *ETS1*. In accordance with findings from previous studies, we found a high correlation of our microarray and quantitative RT-PCR data with correlations of 0.84, 0.81, and 0.86 for *FOXO1A*, *MLL5*, and *ETS1*, respectively (data not shown).

Correlation with clinical and genomic findings

To gain further insight into the significance of new subtypes, we examined the distribution of relevant clinical and molecular genetic parameters among samples. Sex, age, and percentage of bone marrow blasts were evenly distributed between the CBF subclasses group I and II (Table 2). For French-American-British (FAB) subtypes there was a trend toward a correlation of FAB M4 with group I cases ($P = .085$, Fisher exact test), which is likely due to the higher frequency of $inv(16)$ cases in this group ($P = .035$, Fisher exact test). Furthermore, cases in group I displayed higher white blood cell counts (WBCs) ($P = .011$, Fisher exact test); this effect could be mainly attributed to $inv(16)$ cases, which had a higher WBC in group I compared with group II (Table 2). While there was a significant association with loss of one X chromosome copy in females in group II ($P = .019$, Fisher exact test), there was no correlation with secondary chromosome aberrations known to be prognostically relevant in CBF-like loss of the Y chromosome in male $t(8;21)$ cases or trisomy 22 in $inv(16)$ leukemias.^{15,16} There was no correlation with fusion gene transcript levels at diagnosis. Regarding the distribution of molecular aberrations, while *FLT3*-ITDs were more prevalent in group I ($P = .026$, Fisher exact test), there was no significant association of the newly defined groups with *FLT3*-TKD, *KIT*, or *NRAS* mutations (Table 2). Notably, the

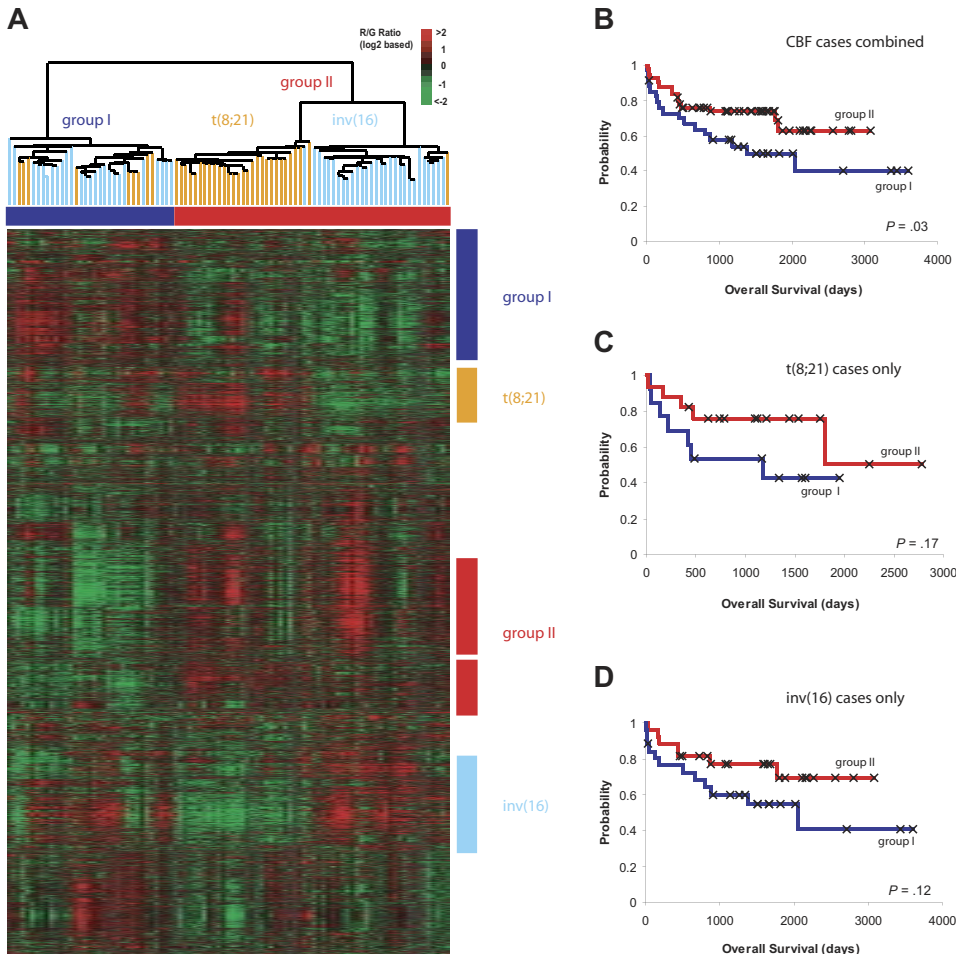


Figure 1. Unsupervised hierarchical cluster analyses. (A) Thumbnail overview of an unsupervised 2-way hierarchical cluster analysis of 93 CBF AML cases (columns) and 856 variably expressed genes (rows). Mean-centered gene-expression ratios are depicted by a \log_2 pseudocolor scale (indicated). Gray denotes poorly measured data. Samples are color-coded according to the cytogenetic groups t(8;21) and inv(16). The sample dendrogram shows that CBF samples separated into 2 major subgroups, as indicated. Gene clusters characterizing the respective groups as well as t(8;21) and inv(16) are highlighted by colored bars. (B) Kaplan-Meier estimates of overall survival in the 2 CBF subgroups; the difference between groups I and II was significant ($P = .029$, log-rank test). The “x” symbols indicate censored data. (C,D) Kaplan-Meier estimates of overall survival of CBF subgroups based on unsupervised hierarchical cluster analysis in t(8;21) (C) and inv(16) cases only (D).

significant association of group I with *FLT3*-ITD was based on only 4 *FLT3*-ITD-positive cases. Thus, the difference between group I and II cannot be fully explained by the presence or absence of *FLT3*-ITDs because these were only found in 14% of group I cases.

Correlation with outcome

Kaplan-Meier analysis identified a statistically significant difference in overall survival (OS) between the 2 subclasses ($P = .03$, stratified for type of CBF, log-rank test; Figure 1B), and a similar difference was observed for the consensus cluster-defined groups ($P = .046$, log-rank test; Figure 2B). Unsupervised hierarchical cluster analyses performed only within the t(8;21) or the inv(16) group revealed t(8;21) and inv(16) clusters corresponding to the subgroups found in the analysis of the combined CBF data set (data not shown). In accordance, the respective subgroups corresponding to group I showed a trend toward inferior outcome ($P = .17$ and $P = .12$, respectively, log-rank test; Figure 1C,D). Correlation of the hierarchical cluster-defined subgroups revealed no statistically significant difference regarding the CIR between groups I and II ($P = .28$, log rank test; Figure S1A), although there were more relapses in group I (15 of 28 in group I versus 18 of 50 in group II, $P = 0.16$, Fisher exact test).

To test whether the difference in OS was independent of type of CBF leukemia and presenting WBC we performed a multivariate proportional hazards analysis. While there was a trend for the hierarchical cluster-derived group II toward better OS (hazards ratio, 0.51; CI, 0.24 to 1.07; $P = .08$), WBC and CBF subtype did not seem to contribute to the differences in outcome ($P = .68$ and $P = .25$, respectively). In addition, we repeated the Kaplan-Meier

estimates of overall survival in the 2 hierarchical cluster-defined CBF subgroups excluding 4 *FLT3*-ITD-positive cases. With the exclusion of these 4 samples, we still observed a trend toward poorer outcome in the remaining group I cases compared with group II ($P = .12$, log-rank test).

The number of younger adults with inv(16) AML who had received an autologous or allogeneic stem cell transplantation as postremission therapy in first complete remission (CR) was equally distributed between group I ($n = 9$) and II ($n = 12$) cases. Nevertheless, we investigated the CIR and CID in the subset of group I and II patients who had received chemotherapy as postremission therapy. While we did not see a significant difference between the hierarchical cluster-defined groups, we however observed a trend ($P = .11$ and $P = .14$ for CIR and CID, respectively, log-rank test; Figure S1B), which is in accordance with our results in the entire cohort.

Characterization of CBF cases by array CGH

To further investigate whether unsupervised hierarchical clustering of our CBF AML cases was driven by as yet unknown secondary aberrations, we performed array CGH experiments for a random subset of 58 samples. High-resolution screening for unbalanced genomic aberrations did not reveal a substantial number of additional recurrent aberrations but allowed us to further define with higher resolution the boundaries of a 9q deletion that had been previously identified by conventional cytogenetic banding analysis. We identified an approximately 9.3 Mb-sized deleted fragment, a del(9)(q21q21) spanning a previously described 2.4 Mb-sized commonly deleted fragment in 9q21⁴⁵ (Figure S2).

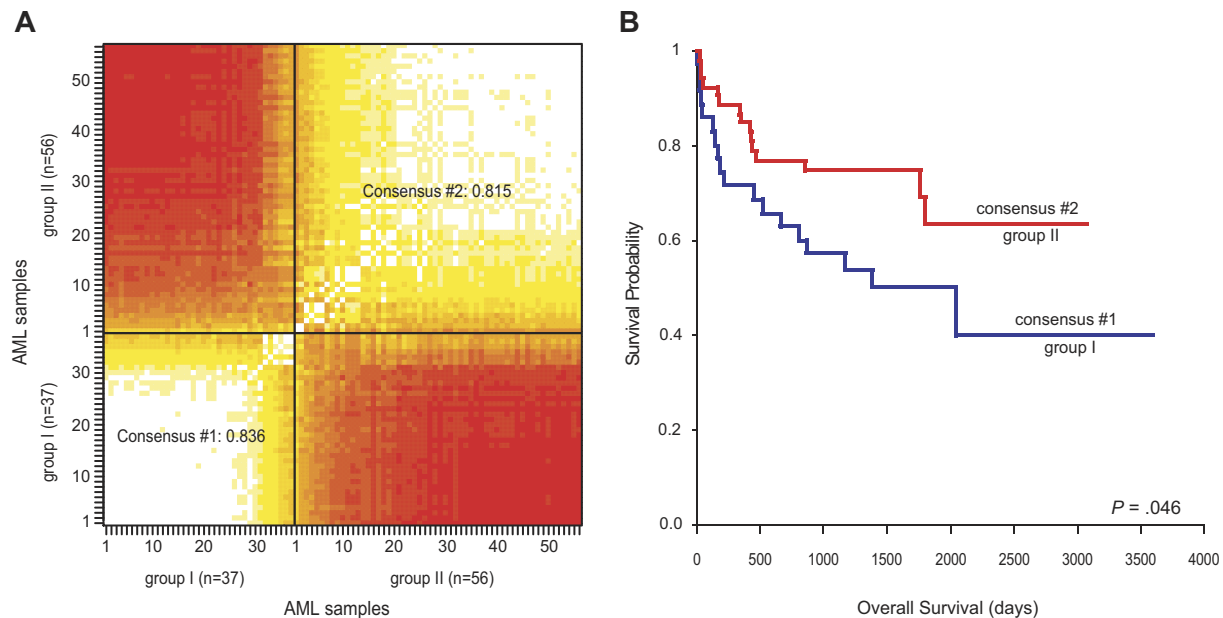


Figure 2. Consensus clustering. (A) For each pair of samples in the unsupervised hierarchical cluster analysis, the R measure (the proportion of the time sample pairs stay in the same cluster during consensus clustering) is indicated for each original cluster as an average over all pairs of samples. The R measures for individual pairs of samples are color-coded with white indicating that a given sample pair clustered 100 times in the same group and red denoting no coclustering. The white diagonal line displays the intraindividual comparison of results for a patient with AML (ie, 100× coclustering). (B) Kaplan-Meier estimates of overall survival in the 2 CBF consensus clusters; the difference between cluster no. 1 and no. 2 was significant ($P = .046$, log-rank test).

CBF leukemia subgroups—biologic insights

Distinct gene-expression signatures underlying the cytogenetic CBF subgroups as well as the novel unsupervised hierarchical cluster-defined subgroups (Figure 1A) were identified using a supervised analytical approach. By using the SAM method we identified more than 1000 genes that significantly correlated with the CBF groups t(8;21) and inv(16) (false discovery rate, less than 0.0001; Table S3). These cytogenetic group-specific signatures basically reflected previous findings,^{19,20} because genes defining the t(8;21) signature included, for example, *POU4F1*, *CAVI*, *HSPG2*, and *TRH*, and in cases with inv(16) we found high-level expression of, for example, *NT5E*, *PTPRM*, *CLIPR-59*, and *SPARC*. In accordance, gene set enrichment analyses (GSEA) for the cytogenetic signatures showed a significant enrichment of genes associated with many GO groups mainly involved in humoral immune response, immune cell activation, as well as receptor-mediated endocytosis and phagocytosis (Table S4).

Using SAM we also identified more than 1000 genes displaying a significant (false discovery rate, less than 0.0001) differential expression among the newly defined CBF subtypes (Figure 3; Table S5). Group I was, for example, characterized by high-level expression of *BRCA1*, *RAD51*, and *CHEK2*, genes involved in the response to DNA damage and in DNA repair.⁴⁶ In accordance, GSEA identified a significant enrichment of genes belonging to the GO category “damaged DNA binding” (Table 3). Furthermore, group I cases were associated with elevated expression of genes belonging to the GO category “nucleoside metabolism” and the pathway “pyrimidine metabolism” (Table 4). In addition, high-level expression of *JUN* and *FOS* among group I cases (Figure 3) suggested a potential role of aberrant MAPK signaling and Jun N-terminal kinase (JNK) signaling pathways, which regulate biologic processes, such as cell differentiation, proliferation, and transformation. In agreement, GSEA identified a significant association with the pathway “MAPK signaling pathway” (Table 4), and many GO categories were associated with proliferation like “cell division” and “M phase of mitotic cell cycle” (Table 3).

Group II CBF cases were characterized by a prominent gene-expression feature with the top SAM gene being the *Rapamycin-insensitive companion of mTOR*, *RICTOR* (Figure 3), encoding a component of the TOR protein complex.⁴⁷ The group II-defining pattern was also characterized by members of pathways downstream of TOR such as *EIF4EBP1* (*eukaryotic translation initiation factor 4E [eIF4E]-binding protein 1*) and *PDPK1* (*phosphoinositide-dependent protein kinase 1*)⁴⁷ as well as upstream-regulators of TOR like *AKT1* (Figure 3). In addition, we observed expression of AKT1 target genes like *FOXO1A*; higher expression levels of antiapoptotic genes like *BIRC3* and *BIRC6* (Figure 3); and significantly lower expression of *PTEN* in group II cases compared with group I (mean of ratios, 1.318 versus 0.805, respectively; $P < .001$). Notably, GSEA identified a significant enrichment of genes belonging to the GO categories “ATP-dependent helicase activity,” “RNA helicase activity,” “mRNA metabolism,” “mRNA processing,” “nuclear mRNA splicing, via spliceosome,” “RNA splicing,” and “RNA polymerase II transcription mediator activity,” suggesting increased translation initiation in this CBF subgroup (Table 3). Furthermore, there was a significant association with the “TNFR1 signaling pathway” and pathways involved in apoptosis and GO categories associated with ubiquitination (Tables 3,4).

CBF leukemia subgroup prediction

Recently, it has been shown by several groups that the cytogenetic AML subgroups with t(8;21) and inv(16) can be predicted at high accuracy based on their characteristic gene-expression signatures.^{20,21} Similarly, in our data 98% of samples were correctly classified using PAM with a sensitivity of 100% and 95.2%, and a specificity of 95.2% and 100% for inv(16) and t(8;21), respectively.

For class prediction of the newly defined, clinically relevant CBF subgroups the PAM algorithm also provided a high cross-validation performance with a sensitivity of 97.1% and 93.1% and a specificity of 93.1% and 100% for group I and group II cases, respectively. The positive predictive value in this cohort was

Table 2. Distribution of factors between hierarchical cluster-defined CBF subgroups

Factors at diagnosis	Group I; n = 35	Group II; n = 58	P
Sex			
Male, no. (%)	19/35 (54)	40/58 (69)	—
Female, no. (%)	16/35 (46)	18/58 (31)	ns
Age			
No. of patients	34	55	—
Median, y (range)	46 (19-72)	47 (19-73)	ns
FAB subtype			
M2 (%)	6/32 (19)	19/53 (36)	ns
M4 (%)	22/32 (69)	25/53 (47)	—
Other (%)	4/32 (12)	9/53 (17)	—
WBC			
No. of patients	32	55	—
Median, $\times 10^9/L$ (range)	42 (2-157)	18 (2-152)	.011
Median in t(8;21), $\times 10^9/L$ (range)	18 (2-130)	12 (2-152)	ns
Median in inv(16), $\times 10^9/L$ (range)	47 (2-157)	29 (2-137)	.057
BM blast			
No. of patients	29	45	—
Median, % (range)	68 (25-100)	70 (6-98)	ns
Cytogenetic group			
t(8;21) (%)	9/35 (26)	29/58 (50)	—
inv(16) (%)	26/35 (74)	29/58 (50)	.035
Additional cytogenetic aberrations			
None (%)	22/34 (65)	25/55 (45)	ns
Trisomy 8 (%)	3/34 (9)	8/55 (15)	ns
del(9q)-9 (%)	1/34 (3)	2/55 (4)	ns
Trisomy 22 (%)	2/34 (6)	4/55 (7)	ns
-Y/males (%)	3/18 (17)	13/38 (34)	ns
-X/females (%)	0/16 (0)	5/17 (29)	.019
Other (%)	6/34 (18)	9/55 (16)	ns
Molecular genetic aberrations			
<i>FLT3</i> -ITD (%)	4/28 (14)	0/52 (0)	.026
<i>FLT3</i> -TKD (%)	4/27 (15)	5/49 (10)	ns
<i>KIT</i> mutation (%)	3/24 (13)	10/41 (24)	ns
Exon 8 (%)	1/24 (4)	5/41 (12)	ns
Exon 17 (%)	2/24 (8)	5/41 (12)	ns
<i>NRAS</i> mutation (%)	5/19 (26)	13/41 (32)	ns
Exon 1 (%)	1/19 (5)	7/41 (17)	ns
Exon 2 (%)	4/19 (21)	6/41 (15)	ns
Fusion gene transcript no. at diagnosis			
No. of patients	19	30	—
Median (range)	52702 (537-11863009)	53746 (6477-1775159)	ns

ns indicates not significant; —, not applicable.

89.5%. Together, these results indicate that the identified signatures might be used to accurately predict the underlying tumor subclasses.

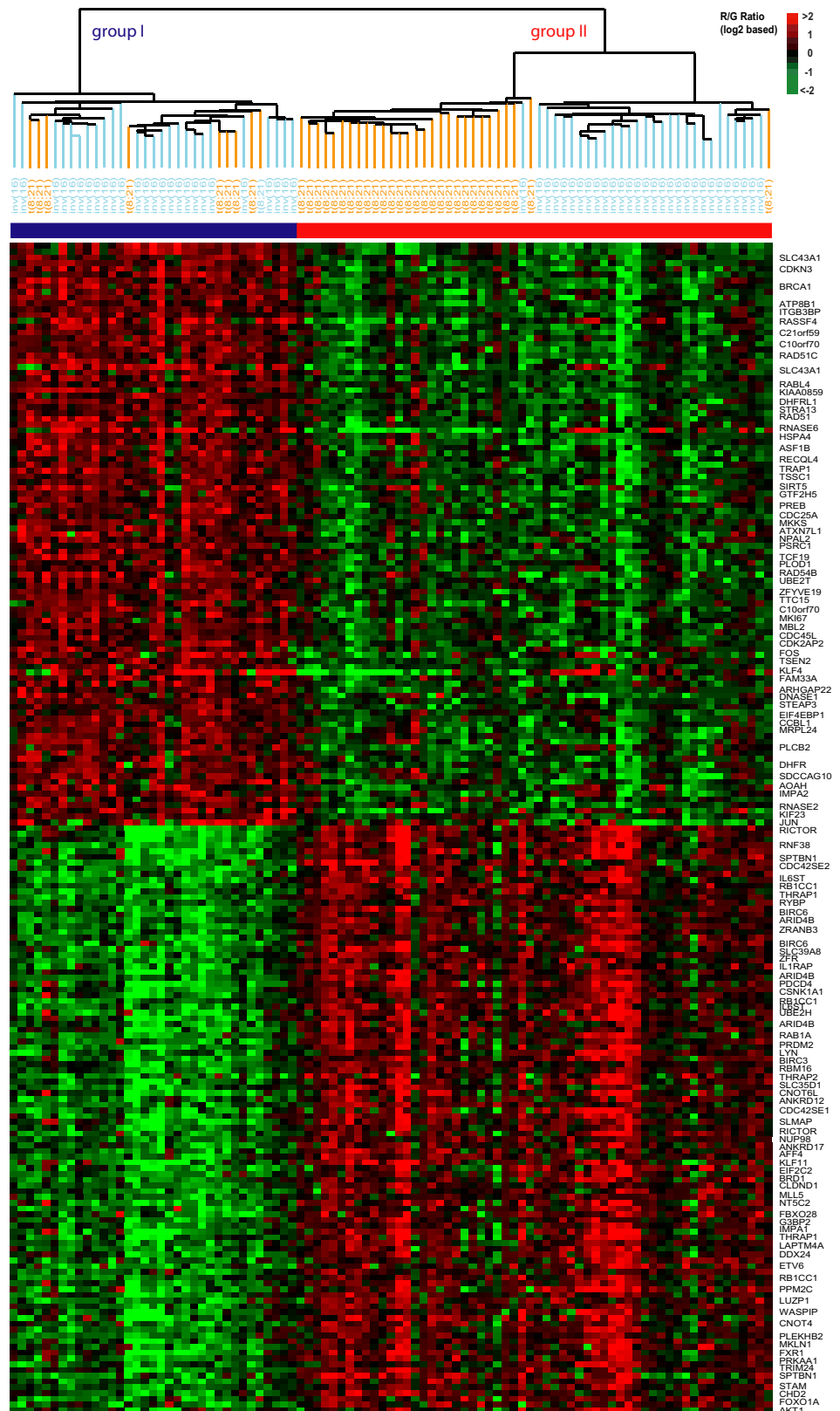
Discussion

In previous analyses, we had observed that samples with t(8;21) and inv(16) each separated into different subgroups based on unsupervised hierarchical clustering.¹⁹ Because the primary translocation events themselves are not sufficient for leukemogenesis,¹⁷ distinct patterns of gene expression found within each of these cytogenetic groups may suggest alternative cooperating mutations and dysregulated pathways leading to transformation. Thus, a major objective of this study was to survey the molecular variation of CBF leukemia in a large set of samples to gain new insight into the underlying biology of these cytogenetic AML groups but, more importantly, to also better understand the clinical heterogeneity we observe in CBF patients. In agreement with previous findings, using unsupervised hierarchical clustering we have discovered that

CBF samples stratify into 2 robust subgroups based on distinct patterns of gene expression.

A significant correlation with WBCs and the unequal distribution of *FLT3*-ITD mutations support distinct biologic behaviors, and the difference in overall survival supports distinct clinical behavior between the newly defined subgroups. While the *FLT3*-ITD cases accounted for only 4 of the 28 AMLs in group I with available *FLT3* mutational status and because we also did not observe a correlation with secondary chromosome aberrations, fusion gene transcript levels, *FLT3*-TKD, *KIT* (exon 8 and 17), and *NRAS* mutations, our findings suggest that the hierarchical cluster-based inv(16)/t(8,21) subgroups reflect yet unknown prognostically relevant pathogenic mechanisms. For group I this mechanism might be similar to the one initiated by *FLT3*-ITD, thereby resulting in increased proliferation that is in part reflected by the elevated WBC in this group. Interestingly, the elevation in the WBC was not just the reflection of an imbalance of inv(16) cases between group I and II but was mainly attributed to higher WBC in inv(16) cases in group I compared with group II. Thus, the

Figure 3. Hierarchical cluster-defined CBF subgroups. Subset of the top SAM genes (rows; ordered by SAM score) characterizing the hierarchical cluster-defined CBF subgroups. Mean-centered imputed gene-expression ratios are depicted by a log₂ pseudocolor scale (indicated). The 93 CBF AML cases (columns) have been ordered according to the dendrogram of the unsupervised 2-way hierarchical cluster analysis (Figure 1). Owing to space limitations, only selected genes are indicated.



Downloaded from <http://ashpublications.net/blood/article-pdf/110/4/1291/479767/zh801607001291.pdf> by guest on 08 June 2024

identification of these new subgroups suggests an improved molecular classification of AML based on gene-expression profiling. Importantly, the genes differentially expressed between the subgroups also provide insight into distinct pathways for the molecular pathogenesis of CBF AML. For example, the newly defined CBF group I was defined by elevated expression of *JUN*

and *FOS*. These genes encode proteins that can form the dimeric AP-1 transcription factor complex that is involved in several “hallmarks” of cancer like tumor cell proliferation and survival of tumor cells.⁴⁸ Thus, overexpression of the proto-oncogene *JUN* and constitutive activation of the JNK and MAPK signaling pathway might be implicated in the leukemic transformation in this CBF

Table 3. GO categories discriminating among hierarchical cluster-defined CBF subgroups

GO description	GO category	No. of genes	LS permutation	KS permutation
Spindle pole	922	22	<.001	<.001
Spindle	5819	34	<.001	<.001
ATP-dependent helicase activity	8026	35	<.001	<.001
DNA-dependent ATPase activity	8094	17	<.001	.021
Small protein conjugating enzyme activity	8639	27	<.001	.006
M phase of mitotic cell cycle	87	96	<.001	<.001
RNA splicing via transesterification reactions	375	51	<.001	<.001
RNA splicing	377	51	<.001	<.001
Nuclear mRNA splicing via spliceosome	398	51	<.001	<.001
mRNA processing	6397	81	<.001	<.001
Mitosis	7067	96	<.001	<.001
RNA splicing	8380	71	<.001	<.001
mRNA metabolism	16071	90	<.001	<.001
Centrosome	5813	20	<.001	.001
Ubiquitin-dependent protein catabolism	6511	47	<.001	.004
Modification-dependent protein catabolism	19941	47	<.001	.004
Ubiquitin conjugating enzyme activity	4840	26	<.001	.008
Dynein complex	30286	11	<.001	.074
Damaged DNA binding	3684	22	<.001	.004
Microtubule organizing center	5815	22	<.001	.002
Cytokinesis	910	92	<.001	.017
Cell division	51301	92	<.001	.017
RNA helicase activity	3724	13	<.001	<.001
Cytoplasmic dynein complex	5868	8	<.001	.033
Ubiquitin-specific protease activity	4843	29	<.001	.01901
Ubiquitin thiolesterase activity	4221	25	<.001	.005
Thiolester hydrolase activity	16790	29	<.001	.006
Microtubule cytoskeleton	15630	79	<.001	.012
Nucleoplasm	5654	93	<.001	.005
Spindle organization and biogenesis	7051	11	<.001	.037
Mitotic spindle organization and biogenesis	7052	11	<.001	.037
Microtubule cytoskeleton organization and biogenesis	226	23	.002	<.001
Microtubule-based process	7017	60	.004	<.001
MAPK	4707	14	.016	<.001
Ribonuclease activity	4540	19	.017	<.001
Gluconeogenesis	6094	9	.034	<.001
Pyruvate metabolism	6090	10	.048	<.001

Number of genes used for random variance estimation: 8556; number of investigated GO categories: 1545; table sorted by *P* value of the LS permutation test; 37 GO categories are significant at the nominal .001 level of the LS permutation test or KS permutation test.

subgroup. Interestingly, elevated *JUN* expression has previously been found in primary AML bone marrow cells of patients with a t(8;21) and inv(16).⁴⁹ Similar to the leukemic effects of *FLT3-ITD*, this mechanism might lead to an increased proliferation. In accordance, CBF group I showed a significant correlation with GO categories associated with proliferation as well as with genes sensing DNA damage and activating DNA repair. In agreement, for example, enhanced *BRCA1* expression has previously been linked to the c-Jun N-terminal kinase (JNK) pathway.^{50,51} *BRCA1* and *RAD51* play a crucial role in DNA repair.⁴⁶ Cells that are defective for *BRCA1* are hypersensitive to agents that produce breaks in double-stranded DNA, and it is thought that the chromosomal instability resulting from loss of *BRCA1* function is a crucial feature of tumorigenesis. However, elevated *BRCA1* expression has on the other hand been demonstrated to lead to an increased resistance against agents or radiation-producing DNA double-strand breaks.⁵²⁻⁵⁴ Thus, increased DNA repair mechanisms might contribute to poorer outcome in group I CBF cases due to “resistance” to DNA double-strand break-inducing agents like idarubicin or etoposide, which also were used for induction chemotherapy in our patients.

PTEN function is attenuated in many tumors through deletion, silencing, or mutation, leading to constitutive activation of AKT⁵⁵

and up-regulation of TOR-dependent pathways.⁴⁷ This might confer a possible mechanism in group II CBF cases that are characterized by elevated expression of *AKT* and mTOR-signaling pathway members. While *PTEN* down-regulates the activity of *PDPK1* and *AKT*, which slows cell growth and induces their accumulation in G₁, it recently has been shown that *RICTOR-mTOR* may be an intriguing target in tumors with impaired expression of *PTEN*, a tumor suppressor opposing *AKT* activation.^{56,57} Notably, a significant enrichment of genes belonging to the GO categories “ATP-dependent helicase activity,” “RNA helicase activity,” “mRNA metabolism,” “mRNA processing,” “nuclear mRNA splicing, via spliceosome,” “RNA splicing,” and “RNA polymerase II transcription mediator activity” supports increased translation initiation in this CBF subgroup. This might possibly be induced by the TOR protein complex, which is a central regulator of both cell growth and proliferation by regulation of translation initiation.⁴⁷

Additional targets for molecular therapies in the newly defined CBF group II include deregulated apoptotic pathways in part reflected by significantly higher expression levels of anti-apoptotic genes like *BIRC3* and *BIRC6*, 2 members of a protein family that inhibits apoptosis by binding to tumor necrosis factor receptor-associated factors.⁵⁸ In agreement, GSEA identified a significant association with the “TNFR1 signaling pathway” and pathways

Table 4. Pathways discriminating among hierarchical cluster-defined CBF subgroups

Pathway description	Pathway ID	No. of genes	LS permutation	KS permutation
MAPK signaling pathway	BioCarta: h_mapkPathway	69	<.001	<.001
Stathmin and breast cancer resistance to antimicrotubule agents	BioCarta: h_stathminPathway	10	<.001	.002
Role of mitochondria in apoptotic signaling	BioCarta: h_mitochondriaPathway	14	<.001	.025
p38 MAPK signaling pathway	BioCarta: h_p38mapkPathway	29	<.001	.022
Caspase cascade in apoptosis	BioCarta: h_caspasePathway	15	<.001	.002
Pyrimidine metabolism	Kegg: hsa00240	38	.001	.003
SODD/TNFR1 signaling pathway	BioCarta: h_soddPathway	9	.002	.021
Bone remodeling	BioCarta: h_rank1Pathway	17	.002	.004
PRC2 complex (long-term gene silencing through modification of histone tails)	BioCarta: h_prc2Pathway	6	.003	.062
FAS signaling pathway (CD95)	BioCarta: h_fasPathway	24	.016	.002
TNFR1 signaling pathway	BioCarta: h_tnfr1Pathway	27	.018	.002
IFN gamma signaling pathway	BioCarta: h_ifngPathway	6	.020	.001
Role of PI3K subunit p85 in regulation of actin organization and cell migration	BioCarta: h_cdc42racPathway	6	.025	.004
Signaling of hepatocyte growth factor receptor	BioCarta: h_metPathway	35	.026	.004
Ceramide signaling pathway	BioCarta: h_ceramidePathway	20	.072	<.001

Number of genes used for random variance estimation: 8556; number of investigated pathways: 233 BioCarta and 76 KEGG pathways (309 total); table sorted by *P* value of the LS permutation test; the first 15 pathways are significant at the nominal .005 level of the LS permutation test or KS permutation test.

involved in apoptosis in this CBF subgroup. Today, an increasing basic understanding of the inhibitor of apoptosis proteins (IAPs) like BIRC3 and BIRC6, which inhibit and modulate cell division, cell cycle progression, and signal transduction pathways,⁵⁹ is being translated into clinically useful applications in the treatment of malignancy. IAPs are attractive therapeutic targets, because they are preferentially expressed in malignant cells, and currently efforts are underway to develop antisense and chemical IAP inhibitors.⁶⁰ In the future, these agents might also be useful for the treatment of this CBF AML subgroup.

In conclusion, while the biologic impact of these signatures in leukemogenesis remains to be validated before novel treatment approaches can be implemented, our findings nevertheless support a clinically useful refined CBF leukemia classification based on gene-expression profiling. Ultimately, the refined molecular characterization of CBF subgroups might provide the means of individualized patient management that will guide an effective combination of both conventional and molecular therapies.

Acknowledgments

This study was supported in part by the Deutsche Forschungsgemeinschaft (BU 1339/2-1), the Deutsche José Carreras Stiftung e.V. (DJCLS R 05/22), and the Leukemia and Lymphoma Society (6151-06).

The authors are indebted to the staff of the Stanford Functional Genomic Facility (SFGF) for providing high-quality cDNA microarrays and to the staff of the Stanford Microarray Database (SMD)

group for providing outstanding database support. For excellent technical assistance we thank Martina Bonenberger, Ursula Botzenhardt, Karina Eiwien, and Marianne Habdank. We also thank all the members of the German-Austrian AML Study Group (AMLSG) for their continuous support of the treatment protocols.

Authorship

Contribution: L.B. and F.G.R. designed and performed research, analyzed and interpreted data, and wrote the paper; S.K., J.D., C.S., S.S., and A.C. performed research and analyzed data; C.L. analyzed and interpreted data and wrote the paper; J.K. and A.G. contributed vital reagents or analytical tools, collected data, and analyzed data; S.F. performed research, analyzed and interpreted data, and wrote the paper; R.F.S. analyzed and interpreted data and wrote the paper; K.D. designed research, analyzed and interpreted data, and wrote the paper; J.R.P. designed research, contributed analytical tools, analyzed and interpreted data, and wrote the paper; and H.D. designed research, contributed vital reagents, analyzed and interpreted data, and wrote the paper.

L.B. and F.G.R. contributed equally to this work.

Conflict-of-interest disclosure: The authors declare no competing financial interests.

Correspondence: Lars Bullinger, Department of Internal Medicine III, University of Ulm, Robert-Koch-Str 8, 89081 Ulm, Germany; e-mail: lars.bullinger@uniklinik-ulm.de.

References

- Grimwade D, Walker H, Oliver F, et al. The importance of diagnostic cytogenetics on outcome in AML: analysis of 1,612 patients entered into the MRC AML 10 trial. The Medical Research Council Adult and Children's Leukaemia Working Parties. *Blood*. 1998;92:2322-2333.
- Slovak ML, Kopecky KJ, Cassileth PA, et al. Karyotypic analysis predicts outcome of pre-remission and postremission therapy in adult acute myeloid leukemia: a Southwest Oncology Group/Eastern Cooperative Oncology Group Study. *Blood*. 2000;96:4075-4083.
- Byrd JC, Mrozek K, Dodge RK, et al. Pretreatment cytogenetic abnormalities are predictive of induction success, cumulative incidence of relapse, and overall survival in adult patients with de novo acute myeloid leukemia: results from Cancer and Leukemia Group B (CALGB 8461). *Blood*. 2002;100:4325-4336.
- Harris NL, Jaffe ES, Diebold J, et al. World Health Organization classification of neoplastic diseases of the hematopoietic and lymphoid tissues: report of the Clinical Advisory Committee meeting-Airlie House, Virginia, November 1997. *J Clin Oncol*. 1999;17:3835-3849.
- Vardiman JW, Harris NL, Brunning RD. The World Health Organization (WHO) classification of the myeloid neoplasms. *Blood*. 2002;100:2292-2302.
- Gao J, Erickson P, Gardiner K, et al. Isolation of a yeast artificial chromosome spanning the 8;21 translocation breakpoint t(8;21)(q22;q22.3) in acute myelogenous leukemia. *Proc Natl Acad Sci U S A*. 1991;88:4882-4886.
- Liu P, Tarle SA, Hajra A, et al. Fusion between transcription factor CBF beta/PEBP2 beta and a myosin heavy chain in acute myeloid leukemia. *Science*. 1993;261:1041-1044.
- Miyoshi H, Shimizu K, Kozu T, Maseki N, Kaneko Y, Ohki M. t(8;21) breakpoints on chromosome 21 in acute myeloid leukemia are clustered within a limited region of a single gene, AML1. *Proc Natl Acad Sci U S A*. 1991;88:10431-10434.
- Speck NA, Gilliland DG. Core-binding factors in

- haematopoiesis and leukaemia. *Nat Rev Cancer*. 2002;2:502-513.
10. Licht JD, Sternberg DW. The molecular pathology of acute myeloid leukemia. *Hematology Am Soc Hematol Educ Program*. 2005:137-142.
 11. Castilla LH, Garrett L, Adya N, et al. The fusion gene Cbfb-MYH11 blocks myeloid differentiation and predisposes mice to acute myelomonocytic leukaemia. *Nat Genet*. 1999;23:144-146.
 12. Okuda T, Cai Z, Yang S, et al. Expression of a knocked-in AML1-ETO leukemia gene inhibits the establishment of normal definitive hematopoiesis and directly generates dysplastic hematopoietic progenitors. *Blood*. 1998;91:3134-3143.
 13. Castilla LH, Ferrat P, Martinez NJ, et al. Identification of genes that synergize with Cbfb-MYH11 in the pathogenesis of acute myeloid leukemia. *Proc Natl Acad Sci U S A*. 2004;101:4924-4929.
 14. Yuan Y, Zhou L, Miyamoto T, et al. AML1-ETO expression is directly involved in the development of acute myeloid leukemia in the presence of additional mutations. *Proc Natl Acad Sci U S A*. 2001;98:10398-10403.
 15. Marcucci G, Mrozek K, Ruppert AS, et al. Prognostic factors and outcome of core binding factor acute myeloid leukemia patients with t(8;21) differ from those of patients with inv(16): a Cancer and Leukemia Group B study. *J Clin Oncol*. 2005;23:5705-5717.
 16. Schlenk RF, Benner A, Krauter J, et al. Individual patient data-based meta-analysis of patients aged 16 to 60 years with core binding factor acute myeloid leukemia: a survey of the German Acute Myeloid Leukemia Intergroup. *J Clin Oncol*. 2004;22:3741-3750.
 17. Frohling S, Scholl C, Gilliland DG, Levine RL. Genetics of myeloid malignancies: pathogenetic and clinical implications. *J Clin Oncol*. 2005;23:6285-6295.
 18. Yan M, Kanbe E, Peterson LF, et al. A previously unidentified alternatively spliced isoform of t(8;21) transcript promotes leukemogenesis. *Nat Med*. 2006;12:945-949.
 19. Bullinger L, Dohner K, Bair E, et al. Use of gene-expression profiling to identify prognostic subclasses in adult acute myeloid leukemia. *N Engl J Med*. 2004;350:1605-1616.
 20. Valk PJ, Verhaak RG, Beijin MA, et al. Prognostically useful gene-expression profiles in acute myeloid leukemia. *N Engl J Med*. 2004;350:1617-1628.
 21. Haferlach T, Kohlmann A, Schnittger S, et al. Global approach to the diagnosis of leukemia using gene expression profiling. *Blood*. 2005;106:1189-1198.
 22. Wilson CS, Davidson GS, Martin SB, et al. Gene expression profiling of adult acute myeloid leukemia identifies novel biologic clusters for risk classification and outcome prediction. *Blood*. 2006;108:685-696.
 23. Schlenk RF, Frohling S, Hartmann F, et al. Intensive consolidation versus oral maintenance therapy in patients 61 years or older with acute myeloid leukemia in first remission: results of second randomization of the AML HD98-B treatment trial. *Leukemia*. 2006;20:748-750.
 24. Frohling S, Schlenk RF, Breitruck J, et al. Prognostic significance of activating FLT3 mutations in younger adults (16 to 60 years) with acute myeloid leukemia and normal cytogenetics: a study of the AML Study Group Ulm. *Blood*. 2002;100:4372-4380.
 25. Frohling S, Skelin S, Liebisch C, et al. Comparison of cytogenetic and molecular cytogenetic detection of chromosome abnormalities in 240 consecutive adult patients with acute myeloid leukemia. *J Clin Oncol*. 2002;20:2480-2485.
 26. Krauter J, Gorlich K, Ottmann O, et al. Prognostic value of minimal residual disease quantification by real-time reverse transcriptase polymerase chain reaction in patients with core binding factor leukemias. *J Clin Oncol*. 2003;21:4413-4422.
 27. Scholl C, Schlenk RF, Eiwien K, Dohner H, Frohling S, Dohner K. The prognostic value of MLL-AF9 detection in patients with t(9;11)(p22;q23)-positive acute myeloid leukemia. *Haematologica*. 2005;90:1626-1634.
 28. Verhaak RG, Goudswaard CS, van Putten W, et al. Mutations in nucleophosmin (NPM1) in acute myeloid leukemia (AML): association with other gene abnormalities and previously established gene expression signatures and their favorable prognostic significance. *Blood*. 2005;106:3747-3754.
 29. Dohner K, Schlenk RF, Habdank M, et al. Mutant nucleophosmin (NPM1) predicts favorable prognosis in younger adults with acute myeloid leukemia and normal cytogenetics: interaction with other gene mutations. *Blood*. 2005;106:3740-3746.
 30. Goemans BF, Zwaan CM, Miller M, et al. Mutations in KIT and RAS are frequent events in pediatric core-binding factor acute myeloid leukemia. *Leukemia*. 2005;19:1536-1542.
 31. Bowen DT, Frew ME, Rollinson S, et al. CYP1A1*2B (Val) allele is overrepresented in a subgroup of acute myeloid leukemia patients with poor-risk karyotype associated with NRAS mutation, but not associated with FLT3 internal tandem duplication. *Blood*. 2003;101:2770-2774.
 32. Ball CA, Awad IA, Demeter J, et al. The Stanford Microarray Database accommodates additional microarray platforms and data formats. *Nucleic Acids Res*. 2005;33:D580-D582.
 33. Eisen MB, Spellman PT, Brown PO, Botstein D. Cluster analysis and display of genome-wide expression patterns. *Proc Natl Acad Sci U S A*. 1998;95:14863-14868.
 34. Rucker FG, Bullinger L, Schwaenen S, et al. Disclosure of candidate genes in acute myeloid leukemia with complex karyotypes using microarray-based molecular characterization. *J Clin Oncol*. 2006;24:3887-3894.
 35. Iafrate AJ, Feuk L, Rivera MN, et al. Detection of large-scale variation in the human genome. *Nat Genet*. 2004;36:949-951.
 36. Sebat J, Lakshmi B, Troge J, et al. Large-scale copy number polymorphism in the human genome. *Science*. 2004;305:525-528.
 37. Rucker FG, Sander S, Dohner K, Dohner H, Polack JR, Bullinger L. Molecular profiling reveals myeloid leukemia cell lines to be faithful model systems characterized by distinct genomic aberrations. *Leukemia*. 2006;20:994-1001.
 38. McShane LM, Radmacher MD, Freidlin B, Yu R, Li MC, Simon R. Methods for assessing reproducibility of clustering patterns observed in analyses of microarray data. *Bioinformatics*. 2002;18:1462-1469.
 39. Tusher VG, Tibshirani R, Chu G. Significance analysis of microarrays applied to the ionizing radiation response. *Proc Natl Acad Sci U S A*. 2001;98:5116-5121.
 40. Tibshirani R, Hastie T, Narasimhan B, Chu G. Diagnosis of multiple cancer types by shrunken centroids of gene expression. *Proc Natl Acad Sci U S A*. 2002;99:6567-6572.
 41. Wright GW, Simon RM. A random variance model for detection of differential gene expression in small microarray experiments. *Bioinformatics*. 2003;19:2448-2455.
 42. Simon R, Lam A. BRB-ArrayTools User Guide, version 3.2. Biometric Research Branch, National Cancer Institute; <http://linus.nci.nih.gov/brb>.
 43. Gray RJ. A class of k-sample tests for comparing the cumulative incidence of a competing risk. *Ann Stat*. 1988;16:1141-1154.
 44. Korn EL. Censoring distributions as a measure of follow-up in survival analysis. *Stat Med*. 1986;5:255-260.
 45. Sweetser DA, Peniket AJ, Haaland C, et al. Deletion of the minimal commonly deleted segment and identification of candidate tumor-suppressor genes in del(9q) acute myeloid leukemia. *Genes Chromosomes Cancer*. 2005;44:279-291.
 46. Narod SA, Foulkes WD. BRCA1 and BRCA2: 1994 and beyond. *Nat Rev Cancer*. 2004;4:665-676.
 47. Bjornsti MA, Houghton PJ. The TOR pathway: a target for cancer therapy. *Nat Rev Cancer*. 2004;4:335-348.
 48. Eferl R, Wagner EF. AP-1: a double-edged sword in tumorigenesis. *Nat Rev Cancer*. 2003;3:859-868.
 49. Elsasser A, Franzen M, Kohlmann A, et al. The fusion protein AML1-ETO in acute myeloid leukemia with translocation t(8;21) induces c-jun protein expression via the proximal AP-1 site of the c-jun promoter in an indirect, JNK-dependent manner. *Oncogene*. 2003;22:5646-5657.
 50. Harkin DP, Bean JM, Miklos D, et al. Induction of GADD45 and JNK/SAPK-dependent apoptosis following inducible expression of BRCA1. *Cell*. 1999;97:575-586.
 51. Potapova O, Haghghi A, Bost F, et al. The Jun kinase/stress-activated protein kinase pathway functions to regulate DNA repair and inhibition of the pathway sensitizes tumor cells to cisplatin. *J Biol Chem*. 1997;272:14041-14044.
 52. Husain A, He G, Venkatraman ES, Spriggs DR. BRCA1 up-regulation is associated with repair-mediated resistance to cis-diamminedichloroplatinum(II). *Cancer Res*. 1998;58:1120-1123.
 53. Abbott DW, Thompson ME, Robinson-Benion C, Tomlinson G, Jensen RA, Holt JT. BRCA1 expression restores radiation resistance in BRCA1-defective cancer cells through enhancement of transcription-coupled DNA repair. *J Biol Chem*. 1999;274:18808-18812.
 54. Quinn JE, Kennedy RD, Mullan PB, et al. BRCA1 functions as a differential modulator of chemotherapy-induced apoptosis. *Cancer Res*. 2003;63:6221-6228.
 55. Vivanco I, Sawyers CL. The phosphatidylinositol 3-kinase AKT pathway in human cancer. *Nat Rev Cancer*. 2002;2:489-501.
 56. Sarbassov DD, Guertin DA, Ali SM, Sabatini DM. Phosphorylation and regulation of Akt/PKB by the rictor-mTOR complex. *Science*. 2005;307:1098-1101.
 57. Yilmaz OH, Valdez R, Theisen BK, et al. Pten dependence distinguishes haematopoietic stem cells from leukaemia-initiating cells. *Nature*. 2006;441:475-482.
 58. Salvesen GS, Duckett CS. IAP proteins: blocking the road to death's door. *Nat Rev Mol Cell Biol*. 2002;3:401-410.
 59. Wright CW, Duckett CS. Reawakening the cellular death program in neoplasia through the therapeutic blockade of IAP function. *J Clin Invest*. 2005;115:2673-2678.
 60. Schimmer AD, Dalili S. Targeting the IAP family of caspase inhibitors as an emerging therapeutic strategy. *Hematology Am Soc Hematol Educ Program*. 2005:215-219.